

# Are T1-Weighted Three-Dimensional Magnetic Resonance Images Inferior to T2-Weighted Images for Diagnosing Lumbar Foraminal Stenosis in the Fifth Lumbar Nerve Root? A Prospective, Comparative Study in Identical Patients

Ko Hashimoto<sup>1,2</sup>, Yasuhisa Tanaka<sup>2</sup>, Takumi Tsubakino<sup>2</sup>, Takeshi Hoshikawa<sup>3</sup>, Chikashi Kawahara<sup>4</sup>, Tomowaki Nakagawa<sup>3</sup>, Satoshi Tateda<sup>5</sup>, Kohei Takahashi<sup>1,2</sup>, Manabu Suzuki<sup>2,4</sup>, Takahiro Onoki<sup>1,6</sup>, Haruo Kanno<sup>7</sup>, Naoki Morozumi<sup>4</sup>, Yutaka Koizumi<sup>4</sup>, Masahito Honda<sup>6</sup>, Takashi Kusakabe<sup>8</sup>, Masaru Suda<sup>9</sup>, Shoichi Kokubun<sup>4</sup> and Toshimi Aizawa<sup>1</sup>

1) Department of Orthopaedic Surgery, Tohoku University Graduate School of Medicine, Sendai, Japan

2) Department of Orthopaedic Surgery, Tohoku Central Hospital, Yamagata, Japan

3) Sendai Orthopaedic Hospital, Sendai, Japan

4) Department of Orthopaedic Surgery, Sendai Nishitaga Hospital, Sendai, Japan

5) Department of Orthopaedic Surgery, Ishinomaki Red Cross Hospital, Ishinomaki, Japan

6) Department of Orthopaedic Surgery, Takeda General Hospital, Aizu-wakamatsu, Japan

7) Department of Orthopaedic Surgery, Tohoku Medical and Pharmaceutical University, Sendai, Japan

8) Department of Orthopaedic Surgery, Tohoku Rosai Hospital, Sendai, Japan

9) Department of Radiology, Tohoku Central Hospital, Yamagata, Japan

## Abstract:

**Introduction:** Imaging analysis of foraminal stenosis in the fifth lumbar (L5) nerve root remains to be a challenge because of the anatomical complexity of the lumbosacral transition. T2-weighted three-dimensional (3D) magnetic resonance images (MRI) have been dominantly used for diagnosis of lumbar foraminal stenosis, while the reliability of T1-weighted images (WI) has also been proven. In this study, we aim to compare the reliability and reproducibility of T1- and T2-weighted 3D MRI in diagnosing lumbar foraminal stenosis (LFS) of the L5 nerve root.

**Methods:** In this study, 39 patients with unilateral L5 radiculopathy (20 had L4-L5 intracanal stenosis; 19 had L5-S foraminal stenosis) were enrolled, prospectively. T1- and T2-weighted 3D lumbar MRI were obtained from each patient. T1 WI and T2WI were blinded and then separately reviewed twice by four examiners randomly. The examiners were instructed to answer the side of LFS or absence of LFS. The correct answer rate, sensitivity, specificity, and area under the curve were analyzed and compared between T1WI and T2WI. Also, intra- and interobserver agreements were calculated using kappa ( $\kappa$ )-statistics and compared in the same manner.

**Results:** The average correct answer rate, sensitivity, specificity, and area under the curve of the T1WI/T2WI were 84.6%/80.1%, 82.9%/80.3%, 86.3%/81.3%, and 0.846/0.801, respectively. The intraobserver  $\kappa$ -values of the four examiners ranged from 0.692 to 0.916 (average: 0.762) and from 0.669 to 0.801 (average: 0.720) for T1WI and T2WI, respectively. The interobserver  $\kappa$ -values calculated in a round-robin manner (24 combinations in total) ranged from 0.544 to 0.790 (average: 0.657) and from 0.524 to 0.828 (average: 0.652), respectively.

**Conclusions:** As per our findings, T1- and T2-weighted 3D MRI were determined to have nearly equivalent reliability and reproducibility in terms of diagnosing LFS of the L5 nerve root.

**Keywords:**

Lumbar foraminal stenosis, fifth lumbar nerve root, three-dimensional MRI, reliability, reproducibility, intraobserver agreement, interobserver agreement

Spine Surg Relat Res 2023; 7(5): 436-442

dx.doi.org/10.22603/ssrr.2023-0026

## Introduction

The lumbar intervertebral foramen was once named as “hidden zone” by Macnab, probably because conventional imaging analyses, such as myelogram, could hardly depict and help diagnose lumbar foraminal stenosis (LFS)<sup>1</sup>. Recently, the lumbar intervertebral foramen became clearly visible, owing to the progress in imaging techniques, such as computed tomography (CT) and magnetic resonance imaging (MRI)<sup>2-12</sup>. In contrast, imaging analysis of foraminal stenosis of the fifth lumbar (L5) nerve root remains to be a challenge because of the individually unique shape of the L5 transverse process, the existence of sacral ala, and the complexed L5 nerve root tract formed by surrounding ligaments and osteophytes<sup>13-16</sup>. To describe the nerve root in the intraforaminal and extraforaminal areas, T2-weighted three-dimensional (3D) MRI has been dominantly used to date<sup>2,4,12</sup>. Meanwhile, T1-weighted imaging clearly outlines the structures bordering the intervertebral foramen, such as the cortex of the pedicle, vertebral body, Sharpey’s fibers in the periphery of the disk, and ligamentum flavum<sup>5,6</sup>. Furthermore, some authors recommend using T1-weighted imaging in diagnosing LFS as it can depict perineural fat obliteration at the lumbar foraminal area<sup>10,17,18</sup>. As per Bezuidenhout et al., foraminal T1 fat hyperintensity provides an ideal background for identifying masses and disk components in foraminal spaces<sup>19</sup>. Therefore, we have been using T1-weighted 3D MRI for diagnosing LFS<sup>20</sup>.

The reliability and reproducibility of T1-<sup>20</sup> and T2-weighted<sup>2,12</sup> 3D MRI in diagnosing LFS have been investigated and proven. However, no study has directly compared T1- and T2-weighted 3D MRI in terms of their ability to diagnose LFS. Thus, this study aims to directly compare the reliability and reproducibility of T1- and T2-weighted 3D MRI using images taken from identical individuals.

## Materials and Methods

### Patients

This study is a prospective, multicenter study conducted by the affiliated hospitals of the Tohoku University Spine Society. In total, 39 patients with unilateral L5 radiculopathy who underwent posterior decompression at the affiliated hospitals from March 2015 to March 2019, achieving immediate neurological pain relief of >50% in visual analog scale after surgery, were included in this study. The diagnosis of

L5 radiculopathy was confirmed based on thorough neurological examination, imaging studies, and selective L5 nerve root block when necessary. These criteria excluded the effect of spontaneous pain relief from lumbar radiculopathy that is empirically considered to take longer time for pain halving; moreover, it was ensured that the site of nerve pathology was definitely identical to the site of decompression surgery. Of the 39 patients, (i) 20 with L4-L5 intracanal stenosis (ICS) underwent ipsilateral L4-L5 intracanal decompression (no-LFS group: control), while (ii) 19 with L5-S foraminal stenosis underwent ipsilateral L5-S extraforaminal decompression (LFS group). Intracanal decompression is a partial laminotomy of the L4-L5 segment, in which a part of the L4 lamina, the medial part of the L4 inferior facet, and the medial part of L5 superior facet are resected, leaving sufficient width of the facet joint, ensuring the decompression of the spinal canal and the exit of the L5 nerve root. Extraforaminal decompression includes a partial resection of the lateral part of the L5 pars interarticularis, the medio-caudal part of the L5 transverse process, and the sacral ala, decompressing the L5 nerve root at the L5-S extraforaminal part<sup>16</sup>. The demographic data of the patients are shown in Table 1. Patients with concomitant ICS and LFS of the identical L5 nerve root (“double crush”), with a previous history of spinal surgeries and without immediate pain relief after the decompression surgery, were excluded from this study. A signed informed consent was obtained from each patient.

### *Coronal and oblique-coronal T1- and T2-weighted 3D MRI*

Preoperative T1- and T2-weighted 3D MRI were obtained using MAGNETOM Avanto<sup>TM</sup>, a 1.5-T scanner with a spinal coil (SIEMENS, Munich, Germany), from identical patients. To obtain T1- and T2-weighted 3D images, the 3D fast low-angle shot and 3D multi-echo data imaging combination gradient echo scan techniques were used, respectively. The precise imaging conditions are shown in Table 2. For both T1- and T2-weighted images (WI), the multiplanar reconstruction method was used to obtain coronal and oblique-coronal images depicting a whole-length image of the bilateral L5 nerve roots from their bifurcation, from the dural sac to the extraforaminal part in one section, on a workstation (Fig. 1). The precise methods for generating whole-length coronal images of the L5 root in a slice are shown in a previous study<sup>20</sup>.

**Table 1.** Demographic Data of the Patients.

	L4-5 intracanal stenosis	L5-S foraminal stenosis
Number of patients (male:female)	20 (6:14)	19 (11:8)
Patients' age (mean±SD)	48–82 (72±9)	37–83 (60±13)

SD: standard deviation

**Table 2.** Scanner Settings for Three-Dimensional Magnetic Resonance Imaging.

Setting element	T1-WI	T2-WI
	Parameter	
Imaging method	3D-FLASH	3D-MEDIC
βOrientation	Coronal	Coronal
Phase encoding direction	R>>L	F → H
Phase oversampling	90%	50%
Slice oversampling	29%	28.6%
Slice per slab	56	56
Flip angle	30°	12°
Base resolution	256	256
Phase resolution	100%	100%
Dimension	3D	3D
PAT mode	GRAPPA×2	GRAPPA×2
FOV	260×191 mm	260×260 mm
Voxel size	1×1×1.2 mm	1×1×1.2 mm
Slice thickness	1.2 mm	1.2 mm
TR	30 ms	38 ms
TE	4.76 ms	14 ms
Fat suppression	Non	Water excitation
Slice resolution	75%	75%
RF spoiling	On	On
Band width	130 Hz/Px	501 Hz/Px
RF pulse type	Normal	Fast
Gradient mode	Normal	Fast
Scan time	5 min 0 sec	5 min 23 sec

WI, weighted image; 3D-FLASH, three-dimensional fast low angle shot; 3D-MEDIC, three-dimensional multiecho data image combination; PAT, parallel acquisition technique; FOV, field-of-view; RF, radiofrequency

### Imaging analysis

Four examiners, who are board-certified orthopedic surgeons with >15 years of experience in spine surgery, judged the foraminal stenosis or compression of the L5 nerve roots by swelling, entrapment, horizontalization, or sharp folding of the root at the foraminal or extraforaminal zone, foraminal or extraforaminal disk herniation, and so on, as indicated in previous studies (Fig. 2)<sup>2,12,21</sup>. The image sets of T1- and T2-weighted 3D MRI were evaluated separately, under the condition that the image data from patients with ICS (no-LFS: control) and LFS are mixed and randomly provided to the examiners without any preliminary clinical information, including the presence or absence of L4-L5 stenosis. The examiners were instructed to answer the side of LFS or absence of LFS as per the nerve root findings only in the fo-

raminal region. The examination was performed twice by each examiner with a considerable interval to exclude any learning effect.

### Statistical analysis

The data obtained from T1- and T2-WI were analyzed separately. Their reliability was evaluated in terms of correct answer rate, sensitivity, and specificity of each examiner and trial and by combining the results of all the reviews conducted by the four examiners (eight reviews in total). Receiver operating characteristic (ROC) analysis was also performed to calculate the area under the ROC curve (AUC). The mean values of the correct answer rate, sensitivity, specificity, and AUC by the ROC analysis in eight reviews were compared between T1WI and T2WI using Wilcoxon signed-rank test. The intra- and interobserver agreements of the imaging study were evaluated using the kappa ( $\kappa$ ) statistics, indicating the extent of agreement between two datasets presented by a serial statistical variable ( $\kappa$ -value)<sup>22</sup>. The strength of agreement was defined by  $\kappa$ -value as follows: <0.00 as poor agreement, 0.00-0.20 as slight agreement, 0.21-0.40 as fair agreement, 0.41-0.60 as moderate agreement, 0.61-0.80 as substantial agreement, and 0.81-1.00 as almost perfect agreement<sup>22</sup>. The intraobserver  $\kappa$ -value was calculated using the two reviews of each examiner. Moreover, the interobserver agreement of eight reviews (two reviews × four examiners) was calculated in a round-robin manner (24 combinations in total). The mean  $\kappa$ -values were calculated for the intra- and interobserver agreements, while Wilcoxon's signed-rank test was used to compare between T1WI and T2WI.

### Results

The correct answer rate of the imaging studies of T1WI and T2WI of the 39 patients with ICS and LFS by eight reviews (two reviews × four examiners) ranged from 82.1% to 89.7% (average: 84.6%) and from 71.8% to 84.6% (average: 80.1%), respectively. The sensitivity of the eight reviews ranged from 78.9% to 89.5% (average: 82.9%) for T1WI and from 73.7% to 89.5% (average: 80.3%) for T2WI. The specificity of the eight reviews ranged from 80.0% to 95.0% (average: 86.3%) for T1WI and from 70.0% to 90.0% (average: 81.3%) for T2WI. The AUC of the eight reviews ranged from 0.820 to 0.896 (average: 0.846) for T1WI and from 0.718 to 0.847 (average: 0.801) for T2WI. AUC was noted to be significantly higher for T1WI ( $P < 0.05$ ). The precise data are shown in Table 3.

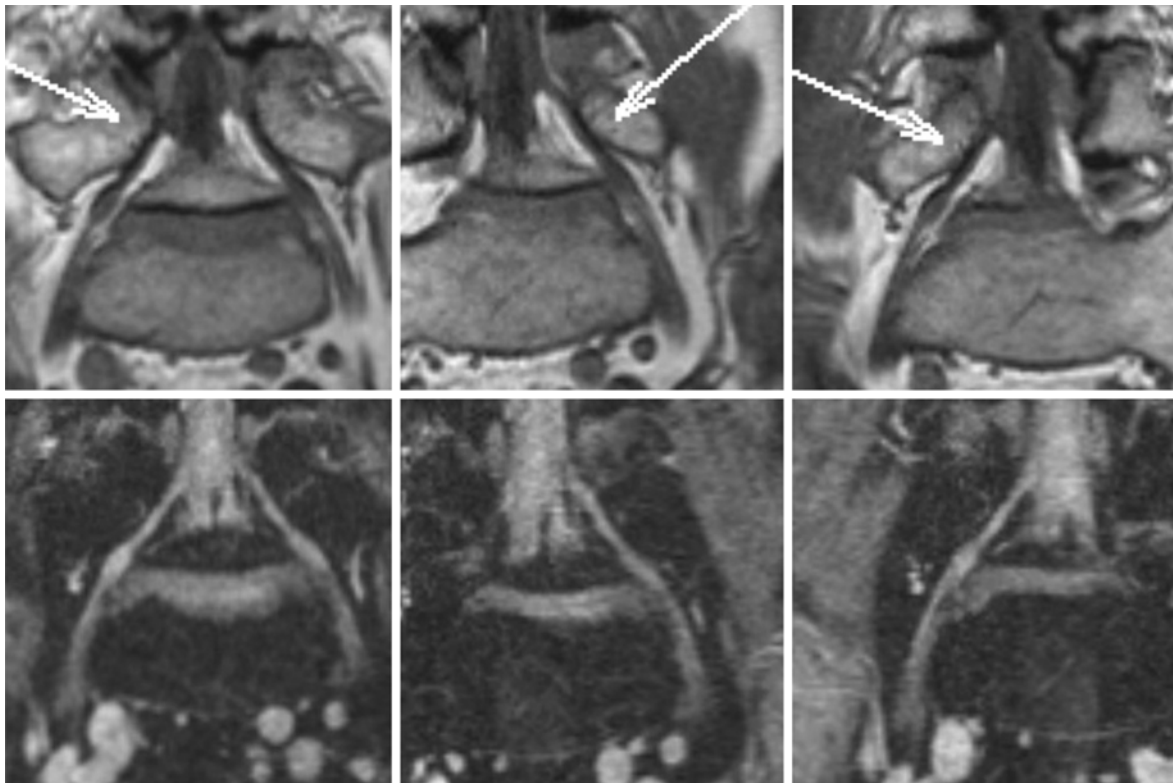


**Figure 1.** T1- and T2-weighted three-dimensional magnetic resonance images (3D MRI) used for this study. Upper row: T1-weighted 3D MRI. Lower row: T2-weighted 3D MRI. Left: coronal section, middle: left oblique-coronal section, and right: right oblique-coronal section.

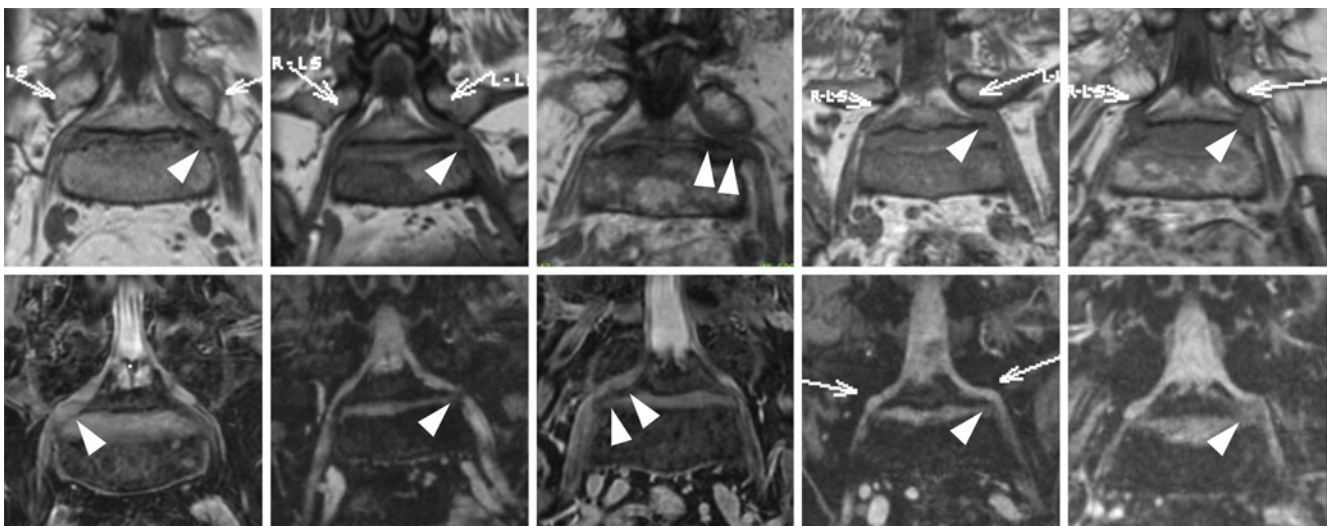


**Figure 2.** Examples of the findings of foraminal stenosis of the L5 nerve root. Upper row: T1-weighted 3D MRI. Lower row: T2-weighted 3D MRI. From left to right: nerve root swelling (arrowhead), nerve root entrapment (arrowhead), nerve root horizontalization (arrowheads), nerve root sharp folding (arrowhead), and extraforaminal disk herniation (arrowhead).

The intraobserver  $\kappa$ -values of the four examiners ranged from 0.692 to 0.916 (average: 0.762) and from 0.669 to 0.801 (average: 0.720) for T1WI and T2WI, respectively. The interobserver  $\kappa$ -values calculated in a round-robin manner (24 combinations in total) ranged from 0.544 to 0.790 (average: 0.657) and from 0.524 to 0.828 (average: 0.652), respectively. All those values showed “substantial agreement.” The precise data of the intra- and interobserver

agreements are demonstrated in Table 4, 5.

### Discussion

In terms of the ability to diagnose LFS, a previous retrospective study demonstrated that T1-weighted 3D MRI had a diagnostic value equivalent to that of T2-weighted 3D MRI<sup>20</sup>. This prospective study is the first to directly com-

**Table 3.** Correct-Answer-Rate, Sensitivity, Specificity, AUC of T1- and T2-Weighted 3D-MRI in Diagnosing L5-S Foraminal Stenosis by Individual Observers.

Examiner	Correct-answer-rate (%) (1 <sup>st</sup> /2 <sup>nd</sup> read)		Sensitivity (%) (1 <sup>st</sup> /2 <sup>nd</sup> read)		Specificity (%) (1 <sup>st</sup> /2 <sup>nd</sup> read)		AUC (1 <sup>st</sup> /2 <sup>nd</sup> read)	
	T1-WI	T2-WI	T1-WI	T2-WI	T1-WI	T2-WI	T1-WI	T2-WI
A	89.7/82.1	71.8/79.5	84.2/78.9	73.7/78.9	95.0/85.0	70.0/85.0	0.896/0.820	0.718/0.795
B	82.1/87.2	82.1/84.6	84.2/84.2	78.9/89.5	80.0/90.0	85.0/80.0	0.821/0.871	0.820/0.847
C	84.6/82.1	76.9/79.5	89.5/84.2	73.7/78.9	80.0/80.0	80.0/80.0	0.847/0.821	0.768/0.794
D	82.1/87.2	84.6/82.1	78.9/78.9	89.5/78.9	85.0/95.0	80.0/90.0	0.820/0.870	0.847/0.820
Average	84.6/84.6	78.8/81.4	84.2/81.6	78.9/81.6	85.0/87.5	78.8/83.8	0.846/0.845	0.788/0.814
Overall average±SD	84.6±3.1	80.1±4.3	82.9±3.7	80.3±6.1	86.3±6.4	81.3±5.8	0.846±0.030*	0.801±0.043

WI, weighted image; SD, standard deviation; \*, significantly higher than T2-WI (p<0.05)

**Table 4.** κ-Values of Intraobserver Agreement.

	T1-WI	T2-WI
Examiner A	0.692	0.801
Examiner B	0.916	0.709
Examiner C	0.797	0.702
Examiner D	0.645	0.669
Average±SD	0.762±0.121	0.720±0.056 <sup>NS</sup>

WI, weighted image; SD, standard deviation; NS, no significant difference with T1-WI

pare the reliability and reproducibility of T1- and T2-weighted 3D MRI in terms of diagnosing LFS. As for reliability in diagnosis, no significant differences with regard to correct answer rate, sensitivity, and specificity were found between T1- and T2-weighted 3D MRI. Therefore, T1-weighted 3D MRI can be used to detect LFS, along with T2-weighted 3D MRI.

The AUC was the only parameter that demonstrated a significant difference between the two imaging modalities, with T1-weighted 3D MRI having the higher value. Therefore, T1-weighted 3D MRI could provide a slightly clearer judgment of LFS than T2-weighted 3D MRI. Presumably, the high specificity of T1-weighted 3D MRI, although not significantly different from that of T2-weighted 3D MRI in this study, could be attributed to its low false-positive rate, resulting in a higher AUC. In fact, Aota et al. reported a relatively higher false-positive rate (48%) in diagnosing L5-S foraminal stenosis using T2-weighted 3D MRI<sup>2)</sup>. The larger AUC for T1WI in this study could be attributed to the relatively lower false-positive rate, presumably based on the fact that perineural fat tissue can be clearly distinguished from its surrounding lesions or disk materials on T1WIs<sup>16)</sup>.

The average κ-values of intra- and interobserver agreements of T1-weighted 3D MRI were 0.762 and 0.657, respectively, whereas those of T2-weighted 3D MRI were 0.720 and 0.652, respectively. The reproducibility of LFS diagnosis using T1WIs and T2WIs was deemed “substantial” and was not significantly different. The results were consistent with the previous retrospective study involving 54 pa-

tients who were assessed by five examiners, demonstrating average κ-values of intra- and interobserver agreements of 0.708 and 0.578, respectively<sup>20)</sup>. Yamada et al. also investigated the reproducibility of L5-S foraminal stenosis diagnosis using T2-weighted 3D MRI, as assessed by three examiners<sup>12)</sup>. The average κ-values of intra- and interobserver agreements were 0.8968 and 0.7988, respectively. In their study, the examiners were informed of the presence or absence of LFS beforehand, which could be the reason why the reliability was higher than that in this study. A previous study also suggested that providing information about the presence or absence of LFS to the examiners increases the intra- and interobserver agreements<sup>20)</sup>.

There are some limitations to be noted in this study. First, the sample size was not large enough to generalize the findings or ideas presented in this study. Moreover, radiologists were not involved in this study as examiners. The reason for this was that spine surgeons are expected to cover all processes or procedures for one patient, from the outpatient department to surgery, including the evaluation of spinal images, in our country. According to our “unique” culture, the examinees were limited to experienced spine surgeons in this study. Furthermore, because of the limited specification of the MRI equipment and the time available for each patient’s scan, the spatial resolution of the images could not be elevated as high-resolution MRI. In some facilities with limited performance of MRI equipment and software, T2-WI can, in principle, take longer to acquire as compared to T1-WI. As patients with LFS often complain of severe leg pain and may not tolerate prolonged supine positioning during MRI imaging, this study suggests that in such cases the T2-WI can be replaced by T1-WI, as the latter has shorter imaging times in diagnosing foraminal stenosis of the fifth lumbar nerve root.

In conclusion, T1- and T2-weighted 3D MRI had nearly equivalent diagnostic reliability and reproducibility in diagnosing LFS of the L5 nerve root. However, it should be noted that the AUC for T1-weighted 3D MRI was larger than that for T2-weighted 3D MRI.

**Conflicts of Interest:** The authors declare that there are

**Table 5.** κ-Values of Interobserver Agreement in Round-Robin Analysis (24 Combinations Each: 4 Examiners×2 Inspections).

T1-WI							
	Ex. A-1 <sup>st</sup>				Average±SD		
Ex. A-2 <sup>nd</sup>	-	Ex. A-2 <sup>nd</sup>			0.657±0.067		
Ex. B-1 <sup>st</sup>	0.621	0.544	Ex. B-1 <sup>st</sup>				
Ex. B-2 <sup>nd</sup>	0.650	0.615	-	Ex. B-2 <sup>nd</sup>			
Ex. C-1 <sup>st</sup>	0.742	0.622	0.715	0.750	Ex. C-1 <sup>st</sup>		
Ex. C-2 <sup>nd</sup>	0.622	0.587	0.715	0.751	-	Ex. C-2 <sup>nd</sup>	
Ex. D-1 <sup>st</sup>	0.691	0.570	0.666	0.611	0.790	0.709	Ex. D-1 <sup>st</sup>
Ex. D-2 <sup>nd</sup>	0.683	0.693	0.574	0.645	0.616	0.578	-

T2-WI							
	Ex. A-1 <sup>st</sup>				Average±SD		
Ex. A-2 <sup>nd</sup>	-	Ex. A-2 <sup>nd</sup>			0.652±0.083 <sup>NS</sup>		
Ex. B-1 <sup>st</sup>	0.637	0.627	Ex. B-1 <sup>st</sup>				
Ex. B-2 <sup>nd</sup>	0.524	0.638	-	Ex. B-2 <sup>nd</sup>			
Ex. C-1 <sup>st</sup>	0.679	0.590	0.828	0.628	Ex. C-1 <sup>st</sup>		
Ex. C-2 <sup>nd</sup>	0.561	0.594	0.786	0.752	-	Ex. C-2 <sup>nd</sup>	
Ex. D-1 <sup>st</sup>	0.564	0.678	0.629	0.678	0.549	0.714	Ex. D-1 <sup>st</sup>
Ex. D-2 <sup>nd</sup>	0.596	0.586	0.738	0.708	0.568	0.784	-

WI, weighted image; Ex., examiner; 1<sup>st</sup>, 1<sup>st</sup> inspection; 2<sup>nd</sup>, 2<sup>nd</sup> inspection; SD, standard deviation; NS, no significant difference with T1-WI

no relevant conflicts of interest.

**Sources of Funding:** None

**Author Contributions:** (I) Conception and design: Ko Hashimoto, Yasuhisa Tanaka, Shoichi Kokubun, Toshimi Aizawa

(II) Administrative support: Yasuhisa Tanaka, Toshimi Aizawa

(III) Provision of study materials and patients: Ko Hashimoto, Yasuhisa Tanaka, Takumi Tsubakino, Yutaka Koizumi, Chikashi Kawahara, Tomowaki Nakagawa, Kohei Takahashi, Manabu Suzuki, Takahiro Onoki

(IV) Collection and assembly of data: Ko Hashimoto, Yasuhisa Tanaka, Takumi Tsubakino, Yutaka Koizumi, Tomowaki Nakagawa, Kohei Takahashi, Manabu Suzuki, Takahiro Onoki, Masahito Honda

(V) Data analysis and interpretation: Ko Hashimoto, Toshimi Aizawa

(VI) Manuscript writing: All authors

(VII) Final approval of manuscript: All authors

**Ethical Approval:** Approval Number: 2014-1-495

The Ethical Committee of Tohoku University Graduate School of Medicine

**Informed Consent:** Informed consent for publication was obtained from all participants in this study.

**References**

1. Macnab I. Negative disc exploration. An analysis of the causes of

nerve-root involvement in sixty-eight patients. *J Bone Joint Surg Am.* 1971;53(5):891-903.

2. Aota Y, Niwa T, Yoshikawa K, et al. Magnetic resonance imaging and magnetic resonance myelography in the presurgical diagnosis of lumbar foraminal stenosis. *Spine.* 2007;32(8):896-903.

3. Byun WM, Jang HW, Kim SW. Three-dimensional magnetic resonance rendering imaging of lumbosacral radiculography in the diagnosis of symptomatic extraforaminal disc herniation with or without foraminal extension. *Spine.* 2012;37(10):840-4.

4. Byun WM, Kim JW, Lee JK. Differentiation between symptomatic and asymptomatic extraforaminal stenosis in lumbosacral transitional vertebra: role of three-dimensional magnetic resonance lumbosacral radiculography. *Korean J Radiol.* 2012;13(4):403-11.

5. Hasegawa T, An HS, Houghton VM. Imaging anatomy of the lateral lumbar spinal canal. *Semin Ultrasound CT MR.* 1993;14(6):404-13.

6. Hasegawa T, Mikawa Y, Watanabe R, et al. Morphometric analysis of the lumbosacral nerve roots and dorsal root ganglia by magnetic resonance imaging. *Spine.* 1996;21(9):1005-9.

7. Heo DH, Lee MS, Sheen SH, et al. Simple oblique lumbar magnetic resonance imaging technique and its diagnostic value for extraforaminal disc herniation. *Spine.* 2009;34(22):2419-23.

8. Kikkawa I, Sugimoto H, Saita K, et al. The role of Gd-enhanced three-dimensional MRI fast low-angle shot (FLASH) in the evaluation of symptomatic lumbosacral nerve roots. *J Orthop Sci.* 2001;6(2):101-9.

9. Lee IS, Kim HJ, Lee JS, et al. Extraforaminal with or without foraminal disk herniation: reliable MRI findings. *AJR Am J Roentgenol.* 2009;192(5):1392-6.

10. Lee S, Lee JW, Yeom JS, et al. A practical MRI grading system for lumbar foraminal stenosis. *AJR Am J Roentgenol.* 2010;194(4):1095-8.

11. Moon KP, Suh KT, Lee JS. Reliability of MRI findings for symptomatic extraforaminal disc herniation in lumbar spine. *Asian*

- Spine J. 2009;3(1):16-20.
12. Yamada H, Terada M, Iwasaki H, et al. Improved accuracy of diagnosis of lumbar intra and/or extra-foraminal stenosis by use of three-dimensional MR imaging: comparison with conventional MR imaging. *J Orthop Sci.* 2015;20(2):287-94.
  13. Ohnishi Y, Yuguchi T, Iwatsuki K, et al. Entrapment of the fifth lumbar spinal nerve by advanced osteophytic changes of the lumbosacral zygapophyseal joint: a case report. *Asian Spine J.* 2012;6(4):291-3.
  14. Matsumoto M, Chiba K, Nojiri K, et al. Extraforaminal entrapment of the fifth lumbar spinal nerve by osteophytes of the lumbosacral spine: anatomic study and a report of four cases. *Spine.* 2002;27(6):E169-73.
  15. Wiltse LL, Guyer RD, Spencer CW, et al. Alar transverse process impingement of the L5 spinal nerve: the far-out syndrome. *Spine.* 1984;9(1):31-41.
  16. Kojo S, Takahashi K, Tsubakino T, et al. Lumbar radiculopathy due to Bertolotti's syndrome: alternative method to reveal the "hidden zone" - A report of two cases and review of literature. *J Orthop Sci.* Forthcoming 2022.
  17. Jenis LG, An HS. Spine update. Lumbar foraminal stenosis. *Spine.* 2000;25(3):389-94.
  18. Yamada K, Abe Y, Satoh S, et al. A novel diagnostic parameter, foraminal stenotic ratio using three-dimensional magnetic resonance imaging, as a discriminator for surgery in symptomatic lumbar foraminal stenosis. *Spine J.* 2017;17(8):1074-81.
  19. Bezuidenhout AF, Lotz JW. Lumbosacral transitional vertebra and S1 radiculopathy: the value of coronal MR imaging. *Neuroradiology.* 2014;56(6):453-7.
  20. Hashimoto K, Tanaka Y, Tsubakino T, et al. Imaging diagnosis of lumbar foraminal stenosis in the fifth lumbar nerve root: reliability and reproducibility of T1-weighted three-dimensional lumbar MRI. *J Spine Surg.* 2021;7(4):502-9.
  21. Hasegawa T, An HS, Haughton VM, et al. Lumbar foraminal stenosis: critical heights of the intervertebral discs and foramina. A cryomicrotome study in cadavera. *J Bone Joint Surg Am.* 1995;77(1):32-8.
  22. Landis JR, Koch GG. The measurement of observer agreement for categorical data. *Biometrics.* 1977;33(1):159-74.

Spine Surgery and Related Research is an Open Access journal distributed under the Creative Commons Attribution-NonCommercial-NoDerivatives 4.0 International License. To view the details of this license, please visit (<https://creativecommons.org/licenses/by-nc-nd/4.0/>).